Bioorganic & Medicinal Chemistry 18 (2010) 5553–5561

Contents lists available at ScienceDirect

Bioorganic & Medicinal Chemistry

journal homepage: www.elsevier.com/locate/bmc

Targeting the ICB2 site of the topoisomerase IIα promoter with a formamido-pyrrole–imidazole–pyrrole H-pin polyamide

Andrew Franks [a], Christopher Tronrud [a], Konstantinos Kiakos [b], Jerome Kluza [b], Manoj Munde [c], Toni Brown [a], Hilary Mackay [a], W. David Wilson [c], Daniel Hochhauser [b], John A. Hartley [b], Moses Lee [a,*]

[a] Division of Natural and Applied Sciences and Department of Chemistry, Hope College, Holland, MI 49423, USA
[b] Cancer Research UK Drug-DNA Interactions Research Group, UCL Cancer Institute, Paul O'Gorman Building, 72 Huntley Street, London WC1E 6BT, UK
[c] Department of Chemistry, Georgia State University, Atlanta, GA 30302, USA

ARTICLE INFO

Article history:
Received 29 April 2010
Revised 9 June 2010
Accepted 14 June 2010
Available online 17 June 2010

Keywords:
Polyamides
DNA
Topoisomerase II
Sequence specificity
Minor groove binders
NF-Y
Gene expression

ABSTRACT

The synthesis, DNA binding characteristics and biological activity of an *N*-formamido pyrrole- and imidazole-containing H-pin polyamide (f-PIP H-pin, **2**) designed to selectively target the ICB2 site on the topoIIα promoter, is reported herein. Thermal denaturation, circular dichroism, isothermal titration calorimetry, surface plasmon resonance and DNase I footprinting studies demonstrated that **2** maintained the selectivity of the unlinked parent monomer f-PIP (**1**) and with a slight enhancement in binding affinity ($K_{eq} = 5 \times 10^5\ M^{-1}$) to the cognate site (5′-TACGAT-3′). H-pin **2** also exhibited comparable ability to inhibit NF-Y binding to **1**, as demonstrated by gel shift studies. However, in stark contrast to monomer **1**, the H-pin did not affect the up-regulation of topoisomerase IIα (topoIIα) in cells (Western blot), suggesting that the H-pin does not enter the nucleus. This study is the first to the authors' knowledge that reports such a markedly different cellular response between two compounds of almost identical binding characteristics.

© 2010 Elsevier Ltd. All rights reserved.

1. Introduction

DNA binding polyamides have shown promise as agents for altering gene expression in living cells, including their use in cancer research and potential application in cancer treatment.[1] Polyamide analogues of the naturally-occurring distamycin A, bind selectively in the minor groove to specific DNA sequences in a 2:1 anti-parallel stacked dimer motif, in which the two oligopeptides are aligned in a staggered manner.[2]

Among the polyamides previously synthesized by the authors, f-PIP [formamido (f)-pyrrole (P)–imidazole (I)–pyrrole (P), **1**, Figure 1A] has been shown to elicit a targeted biological response.[3] Polyamide **1** was designed to target the sequence 5′-TACGAT-3′ (TACGAT) found on the 5′-flank of the inverted CCAAT box-2 (ICB2) in the promoter region of the topoisomerase IIα (topoIIα) gene (Fig. 1B). In confluent cancer cells, nuclear factor-Y (NF-Y) binds to this sequence causing down-regulation of topoIIα.[4,5] This results in the reduced efficacy of anti-cancer therapeutic agents designed to exploit the increased activity of this enzyme.[6] Previous studies in confluent cancer cells demonstrated that compounds which inhibit NF-Y binding to ICB2, are capable of up-regulating topoIIα and sensitizing such cells to the effects of the topoIIα poison, etoposide.[6–8] However, these compounds were found to target additional sites, and this lack of specificity limited further development. Polyamide **1** was thus designed to selectively bind to the 5′-flank of ICB2. Biophysical and in vitro biological testing confirmed that polyamide **1** bound to its target site and subsequently increasing expression of topoIIα in confluent cancer cells.[3] However, the binding affinity of **1**, as determined by surface plasmon resonance (SPR)[9] was reduced as compared to the parent distamycin (K_{eq} = 10^5 vs $10^7\ M^{-1}$, respectively), leaving scope for development.

In an attempt to improve the binding affinity of f-PIP (**1**), yet retain its selectivity, compound **2** (Fig. 1A) was designed, and its synthesis and evaluation are reported herein. The rationale for the design of **2** is that by tethering the two f-PIP monomers together in an 'H-pin' motif, the entropy cost of arranging two un-tethered polyamides within the minor groove is minimized.[10–12] Recent studies from our laboratories demonstrated that H-pin **3**, in which two f-IPI monomers were tethered by an ethylene glycol (EG) moiety, provided an effective molecular design. The favorable solubility of H-pin **3** in aqueous buffer was retained with reference to the non-tethered parent monomer f-IPI (**4**, Fig. 1A), as was sequence selectivity. Additionally, the binding affinity of **3** was dramatically improved ($K_{eq} = 2 \times 10^{10}$ vs $1.9 \times 10^8\ M^{-1}$).[9,10] Thus the H-pin design offers a strategy for designing

* Corresponding author. Tel.: +1 616 395 7190; fax: +1 616 395 7923.
E-mail address: lee@hope.edu (M. Lee).

0968-0896/$ - see front matter © 2010 Elsevier Ltd. All rights reserved.
doi:10.1016/j.bmc.2010.06.041

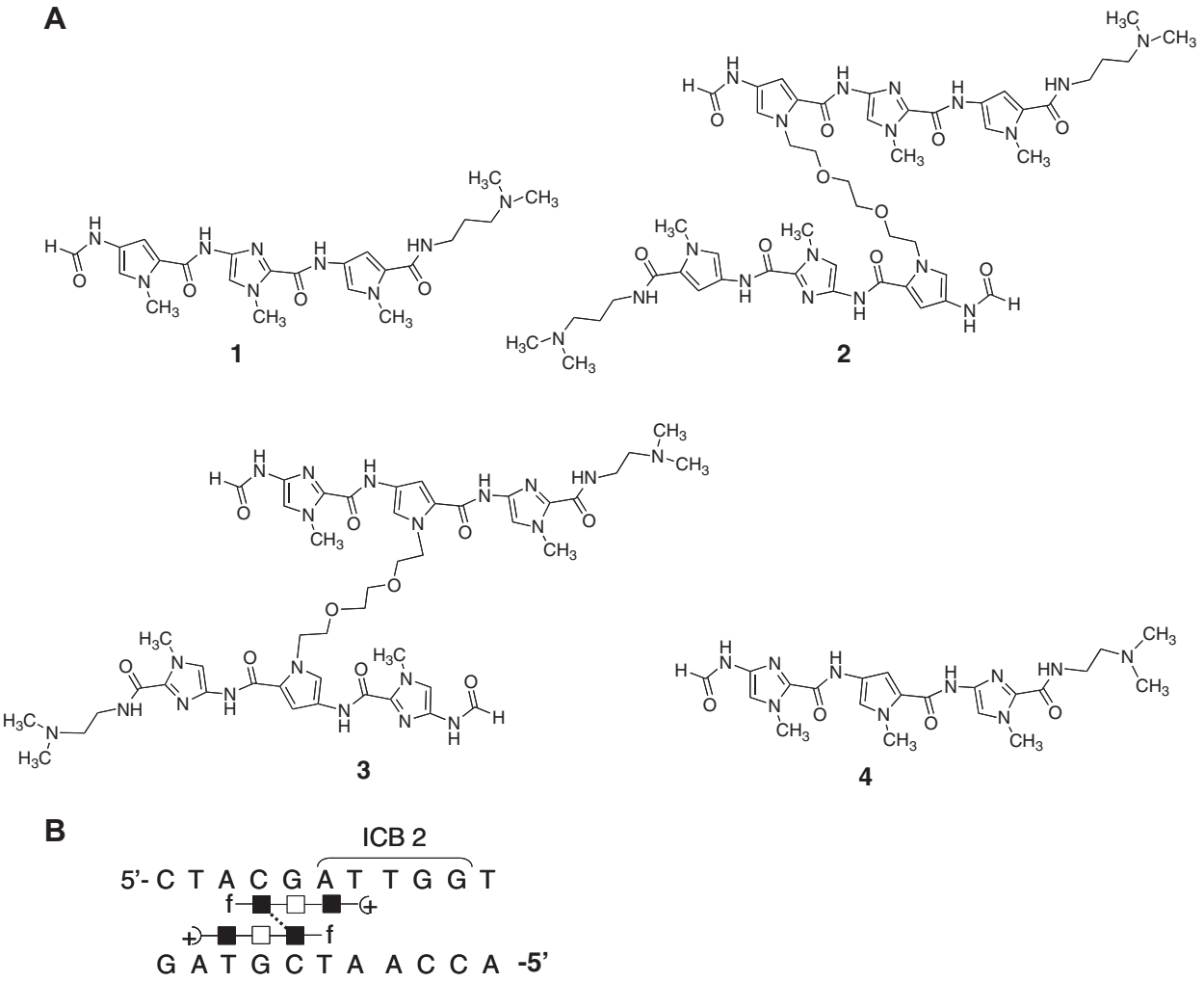

Figure 1. (A) f-PIP monomer **1** and corresponding H-pin **2**, which bind, respectively, in a 2:1 or 1:1 stoichiometric ratio to the 5′-TACGAT sequence on the 5′-flank of the ICB2 site. Analogous polyamides f-IPI H-pin (**3**) and f-IPI (**4**), previously synthesized by the authors' laboratory. (B) Diagram of the ICB2 site, detailing the cognate sequence of H-pin **2**.

new sequence specific polyamides with potential use in controlling gene expression. Accordingly, the f-PIP monomers of H-pin **2** were linked by an EG tether; with the difference that the monomers were joined through the N-terminal P units rather than in the central I position for synthetic reasons. Upon synthesis of f-PIP H-pin **2**, the aim of the current report was to ascertain its binding affinity to the cognate sequence located at the 5′-flank of the ICB2 site (TACGAT), and to determine if **2** was able to inhibit NF-Y binding and, thereby induce expression of the topoIIα gene in confluent cells. The studies were conducted in comparison to the monomer unit f-PIP **1**.

2. Results and discussion

2.1. Synthesis

H-pin **2** was synthesized as described in Scheme 1, adapting a previously published procedure.[12a] The nitro-IP diamide **5** was reduced to the amine via catalytic hydrogenation over palladium on carbon (Pd/C, 5%).[13] The nitro-pyrrole-EG-linked diacid (**6**) was converted to a diacid chloride using thionyl chloride, which was subsequently coupled to the aforementioned amine using Schotten–Baumann chemistry.[14] The resulting nitro-linked-triamide **7** was reduced with 10% Pd/C, and the amine reacted with freshly prepared formic acetic anhydride to produce the final H-pin (**2**) in 16% yield after purification using silica gel column chromatography.[15] Compounds **7** and **2** were characterized by 400 MHz ^{1}H NMR, MS, and FT-IR. The purity of H-pin **2** was ascertained through TLC and ^{1}H NMR analyses.

2.2. Circular dichroism (CD)

When a non-chiral ligand, such as a polyamide, binds in the minor groove of DNA, the resulting chiral complex induces a CD response at ~330 nm.[16] CD studies were carried out using three DNA sequences: cognate sequence TACGAT representing the 5′-flank of the ICB2 site, an A/T rich non-cognate AAATTT, and a second cognate sequence ATCGAT, which differs only in the order of the first two base pairs. It is known that an f/P pairing and the charged dialkylamino tail moiety show no binding preference for A/T over T/A, thus, both cognate sequences should present similar binding sites.[9,17,18] Strong DNA-induced CD bands shown in Figure 2A and B provide evidence that H-pin **2** binds in the minor groove of both cognate sequences. Specifically, ATCGAT was saturated at 20 mdeg ellipticity with 1 molar equiv of added polyamide (Fig. 2A, inset). This 1:1 molar ratio, as well as the appearance of an isodichroic point, indicates that only the desired minor groove binding was observed for the H-pin. In contrast, the AAATTT complex showed a weak response at 3 mdeg with 6 molar equiv of ligand (Fig. 2C). This is typically the observed result when a poly-

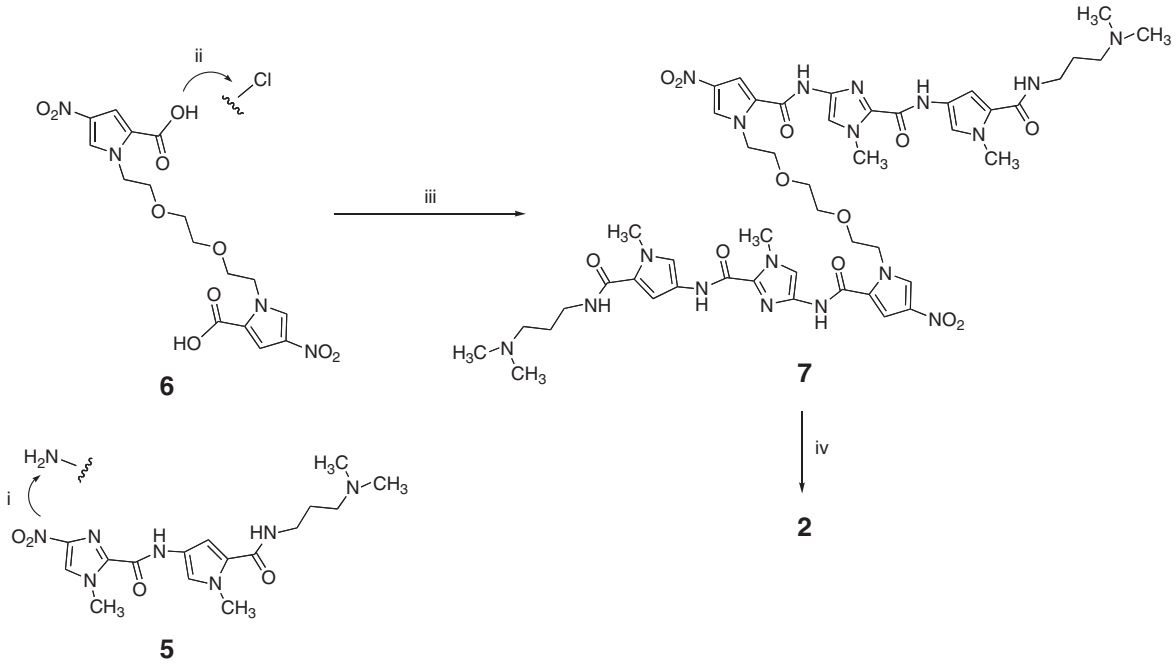

Scheme 1. Reagents and conditions: (i) 5% Pd/C, H_2, cold MeOH, rt, ~24 h; (ii) $SOCl_2$, dry THF, reflux, ~15 min; (iii) dry DCM, dry TEA, 0 °C to rt, ~18 h; (iv) 10% Pd/C, H_2, cold MeOH, rt, ~18 h; (v) formic acetic anhydride, dry DCM, 0 °C to rt, ~18 h.

amide does not interact appreciably with a DNA sequence.[3,13,16,19] Therefore, H-pin **2** was deduced to not only bind in the minor groove, but also to do so selectively.

2.3. Thermal denaturation (ΔT_m)

The difference in the melting temperature (ΔT_m) of ligand-bound and free DNA provides an indication of the binding affinity of polyamides with a particular DNA sequence.[20] Binding of H-pin (**2**) to cognates ATCGAT and TACGAT was proven by ΔT_m values of 6 and 3 °C, respectively (Table 1). These results are complementary to the CD results, with **2** binding to both cognates, but with slightly more affinity to ATCGAT. However, addition of H-pin **2** to the non-cognate AAATTT experiment also demonstrated binding, producing a ΔT_m of 4 °C. This appears somewhat anomalous, but has been observed previously by this group.[10,21]

2.4. Isothermal titration calorimetry (ITC)

ITC provides an effective method to characterize the thermodynamics of ligand–DNA interactions.[22,23] Titration of H-pin **2** to both cognate sequences showed the interactions to be exothermic with enthalpies (ΔH) at 25 °C of −2.7 and −2.8 kcal mol^{-1}, for ATCGAT and TACGAT, respectively (Table 1). The thermogram for the titration of H-pin **2** to ATCGAT is depicted in Figure 3A. In contrast, and consistent with CD studies, titration of H-pin **2** to the non-cognate AAATTT sequence did not show any heat of reaction (Fig. 3B).

2.5. Surface plasmon resonance (SPR)

Accurate binding constants (K_{eq}) and an evaluation of binding kinetics of ligand–DNA interactions can be ascertained from SPR biosensor experiments.[24] H-pin **2** was tested against cognate sequence ATCGAT, non-cognate AT sequence, AAATTT, and a non-cognate GC sequence, ACCGGT. No evidence of binding was observed for the titration of H-pin **2** to the non-cognate sequences (up to 4 μM, data not shown), yet clear interactions were observed for the cognate sequence (Fig. 4A). As is evident, strong binding was observed in the sensorgrams and rates of association are rapid (<0.1 s). SPR studies using the same biosensor chip were simultaneously conducted on the monomer f-PIP **1** (Fig. 4B) with similar concentrations. H-pin **2**, which has roughly twice the molecular weight as that of f-PIP, binds as a monomer to ATCGAT whereas f-PIP binds as a dimer. Hence the predicted RUs (response units) for binding of one molecule of H-pin **2** to ATCGAT are expected to be approximately equal to binding of two molecules of f-PIP. In the comparison of binding plots in Figure 4, f-PIP has fewer RUs in the initial concentration range because its binding affinity is lower than for H-pin **2**. A higher concentration of f-PIP would be needed to match RUs of H-pin 2. K_{eq} for H-pin **2** was calculated using a 1:1 steady state model[10,24] and was found to be 5×10^5 M^{-1}. The observed free energy of the interaction was favorable, with a ΔG value at 25 °C of −7.8 kcal mol^{-1} (Table 1). Using the enthalpy value of −2.8 kcal mol^{-1} determined from ITC studies, the $T\Delta S$, or entropy term, was calculated to be 5.0 kcal mol^{-1}. Hence, the primary thermodynamic driving force for the binding of H-pin **2** to ATCGAT was through gains in entropy. Unexpectedly, this is only a slight enhancement in binding affinity by using the H-pin motif when compared to that of the f-PIP **1** monomer which forms a cooperative 2:1 complex as expected [$K_{eq} = (K_1 \times K_2)^{1/2} = 2 \times 10^5$ M^{-1}; this is the binding constant per molecule to compare directly with the H-pin]. It is worthy to note that the K_{eq} for the monomer f-PIP **1** is in agreement with previously published values.[3] This small enhancement is contrary to our previous findings of using the H-pin motif to enhance binding affinity.

2.6. DNase I footprinting

DNase I footprinting was used to examine the competitive selectivity of H-pin **2** for cognate sites placed within a single DNA fragment containing several cognate and non-cognate sites. Figure 5 shows the titration results for H-pin **2** and f-PIP monomer **1**. A clear footprint is observed for both compounds over the cognate site 5′-AACGAT at 2 μM. However, at 1 μM of H-pin **2** the bands corresponding to this binding site were diminished compared to monomer **1**, indicating that the H-pin gave a slightly stronger affinity. This result is concurrent with the SPR data.

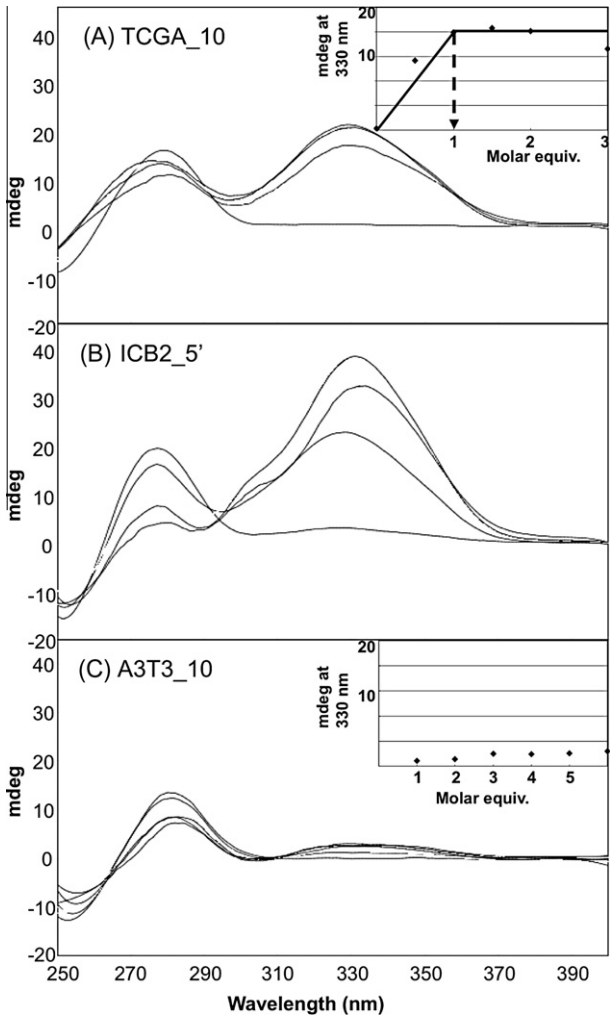

Figure 2. CD spectra for H-pin **2** binding to cognate sites ATCGAT (A) and TACGAT (B), and non-cognate AAATTT (C). Inset graphs show stoichiometric data; the necessary molar equivalents of polyamide–DNA to achieve saturation of the CD signal at 330 nm.

2.7. Electrophoretic mobility shift assay (EMSA)

EMSA can provide direct evidence for the ability of small molecules to interfere with the binding of transcription factors to target DNA sequences. As shown in Figure 6, pre-incubation of H-pin **2** with the radioactive probe containing the ICB2 target sequence, for 1 h and subsequent addition of nuclear extracts from confluent NIH 3T3 cells results in inhibition of NF-Y binding at drug concentrations greater than 3 μM. The same experiment was repeated with the nuclear extracts incubated with the radioactive probe first, for 1 h, before addition of **2**. The NF-Y binding inhibition patterns were identical (data not shown) suggesting that **2** can not only compete but also displace protein factors bound to DNA, including NF-Y, as confirmed by supershifting with antibody to the A subunit of NF-Y.

2.8. Western blot

In order to demonstrate whether H-pin polyamides could be developed as cellular gene control agents, the ability of H-pin **2** to enter the nucleus of cells and subsequently affect gene expression was investigated using immunoblotting. Confluent NIH 3T3 cells were incubated with up to 80 μM H-pin for 4, 6, and 24 h. Western blot analysis of treated cells was performed and the results are shown in Figure 7. Disappointingly, the results demonstrate that H-pin does not affect topoIIα protein expression. This is in contrast to the monomer, f-PIP **1**, which at 10 μM increased topoIIα levels after only 4 h incubation.[3] As a control, the level of lamin in the cells were probed, and it was found to be unaffected (Fig. 7). This indicates that the cells were growing properly and the gene expression machinery was not impaired. It is suggested that due to the bulk of the H-pin, uptake into the nucleus does not occur. This suggestion is supported by recent reports indicating that cell permeability and nuclear localization of hairpin and H-pin polyamides are not predictable, and molecular size and pyrrole/imidazole content are possible determining factors.[25] However, the results do not rule out the possibility that binding of H-pin **2** to albumin or other components might have also blocked any biological activity.

2.9. Cytotoxicity studies

The cytotoxicity of f-PIP H-pin **2** in murine leukemia (L1210) and murine melanoma (B16) cell lines was determined using a colorimetric MTT assay. It was anticipated that **2** would not bear any inherent cytotoxicity as its mechanism of inhibiting NF-Y and up-regulating topoIIα, should not reduce/inhibit cell growth. H-pin **2** was incubated with each cell line over a concentration gradient for 72 h, at which point the MTT stain was added. After 4 h development time, the absorbance of each plate was read and an IC_{50} value (the concentration of **2** required to inhibit 50% cell growth, compared to an untreated control) of >100 μM was determined. Thus, H-pin **2** yields no observable cytotoxicity, even at high concentrations, which is consistent with our hypothesis.

3. Conclusion

The proven success of the H-pin motif to enhance binding affinity of polyamides to cognate DNA sequences was combined with the biological potential of monomeric f-PIP **1** to up-regulate expression of topoIIα, resulting in the design of glycol linked H-pin **2**. H-pin **2** demonstrated excellent solubility in aqueous buffer, gave appreciable DNA binding affinity in the minor groove, and displayed DNA sequence selectivity. H-pin **2** was also shown to inhibit NF-Y from binding to ICB2 at a concentration of 3 μM. However, in contrast to the f-PIP monomer **1**, H-pin **2** had no effect on the up-regulation of topoIIα in a culture of NIH 3T3 cells, suggesting that **2** did not enter the nucleus, presumably due to its bulk. In spite of this outcome, the study still demonstrates the potential of

Table 1
Thermodynamic and biophysical values obtained from thermal denaturation, SPR, and ITC experiments for the interaction of the H-pin **2** with ATCGAT, TACGAT, and AAATTT

DNA	T_m	SPR		ITC	
	ΔT_m (°C)	K_{eq} (M^{-1})	ΔG (kcal mol^{-1})	ΔH (kcal mol^{-1})	$T\Delta S$ (kcal mol^{-1})
ATCGAT	6	5×10^5	−7.8	−2.8	5.0
TACGAT	3	Not determined		−2.7	Not determined
AAATTT	4	No binding observed		No heat observed	

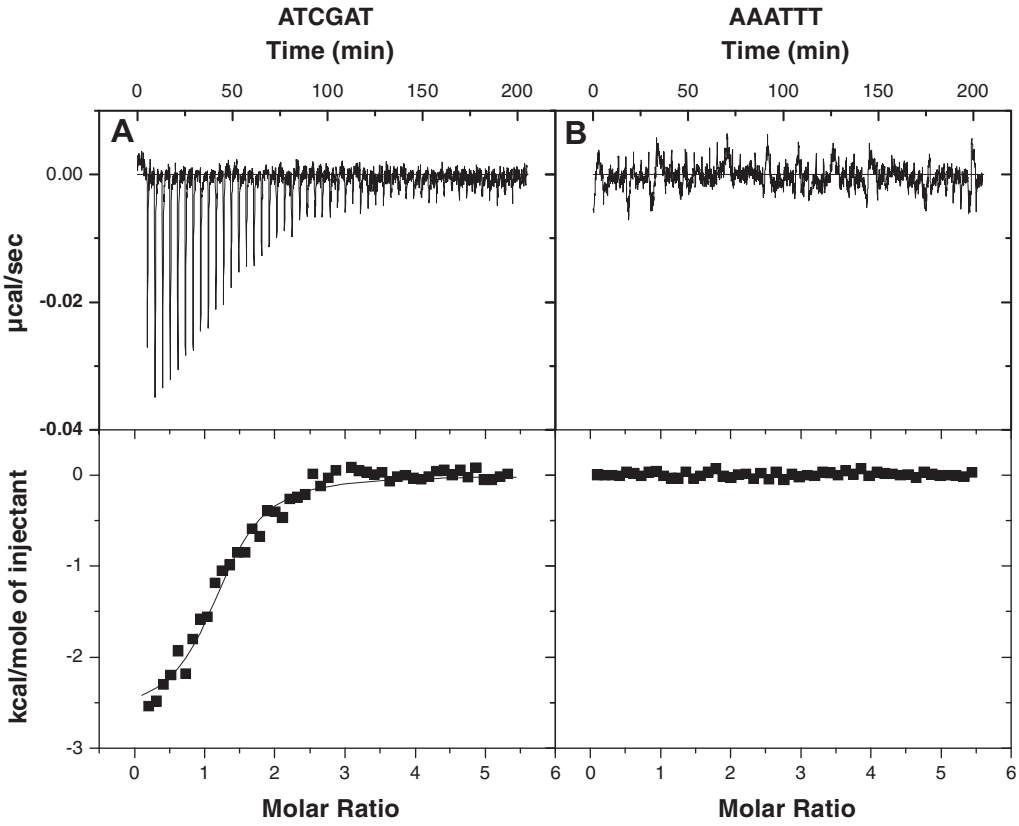

Figure 3. ITC thermograms for H-pin **2** binding to cognate ATCGAT (A) and non-cognate AAATTT (B) at 25 °C.

polyamides to selectively bind predetermined DNA sequences with appreciable affinity. This result is interesting in that it directly compares a monomer and an H-pin that, despite having similar binding characteristics, demonstrate such vastly different cellular properties. Studies currently ongoing in the authors' laboratory are focused on addressing the problem of nuclear uptake through the design of next generation polyamides.

4. Experimental

4.1. Synthesis

4.1.1. General

Solvents and organic reagents were purchased from Aldrich or Fisher Scientific; most products were used without further purification with the exception of DCM and DMF, which were distilled over P_2O_5 and BaO, respectively, prior to use. Melting points were obtained using a Mel-temp melting point apparatus and are uncorrected. Infrared (IR) spectra were recorded using a Midac M1700 FT-IR instrument as films on NaCl plates. ^{1}H NMR spectra were acquired with a Varian Inova 400 MHz instrument. Chemical shifts (δ) are reported at 20 °C in parts per million (ppm) downfield from internal tetramethylsilane (Me_4Si). Mass spectra were provided by the Mass Spectrometry Laboratory, University of South Carolina, Columbia. Reaction progress was assessed by thin-layer chromatography (TLC) using silica gel on aluminum plates (Sorbent Technologies). Visualization was achieved with UV light at 254 nm and/or 366 nm.

4.1.2. Compound 7

Compound **5** (300 mg, 0.79 mmol) was reduced with H_2 in the presence of 5% Pd/C (150 mg) in cold MeOH (~30 mL) for ~24 h at rt.[14] The reaction mixture was filtered through Celite and the catalyst was thoroughly rinsed with MeOH. The MeOH was removed and residual solvent was removed by co-evaporation with DCM (3 × 2 mL). The resulting yellow, solid amino product was protected from light and dried under high vacuum until required. Separately, diacid **6** (162 mg, 0.38 mmol) was dissolved in dry THF (2 mL) and $SOCl_2$ (4 mL) was added to the solution. The reaction mixture was refluxed for ~15 min and then allowed to cool to room temperature. The solvents were removed by aspiration and residual solvent was removed by co-evaporation with dry DCM (3 × 2 mL). The acid chloride was dissolved in DCM (5 mL) and added drop-wise to the above amine in dry triethylamine (TEA) (79.9 mg ≡ 0.06 mL, 0.79 mmol) and dry DCM (~10 mL) at 0 °C (ice/H_2O). The reaction was allowed to warm to rt and was stirred for ~18 h, protected from light. A basic aqueous work-up was performed[24] and the residue purified by flash column chromatography (silica gel, gradient: 100:0:0–0:100:0–95:4.5:0.5 $CHCl_3$/MeOH/NH_4OH) to yield compound **7** as a yellow solid (102 mg, 25%). mp dec 186 °C: R_f 0.12 (69.5:30:0.5% $CHCl_3$/MeOH/NH_4OH); ^{1}H NMR: 400 MHz, CD_3OD, 7.88 (d, J = 1.6 Hz, 2H); 7.38 (d, J = 2.0 Hz, 2H); 7.37 (s, 2H); 7.17 (d, J = 1.6 Hz, 2H); 6.77 (d, J = 2.0 Hz, 2H); 4.55 (t, J = 4.6 Hz, 4H); 3.99 (s, 6H); 3.84 (s, 6H); 3.76 (t, J = 4.0 Hz, 2H); 3.55 (s, 4H); 2.40 (t, J = 8.0 Hz, 4H); 2.25 (s, 12H); 1.76 (quintet, J = 8.0 Hz, 4H); IR (neat) ν 2926, 1660, 1650, 1642, 1632, 1548, 1503, 1434, 1322, 1117 cm^{-1}; MS (ES+) m/z (rel. intensity) 1086 (M+H, 10%); 558 (15%); 543 (100%).

4.1.3. f-PIP-EG H-pin 2

Compound **7** (102 mg, 0.094 mmol) was reduced with H_2 in the presence of 10% Pd/C in cold MeOH for ~18 h at rt.[14] The amine was isolated as above and then re-dissolved in dry DCM (5 mL). Formic acetic anhydride was prepared fresh as previously described.[16] and added drop-wise to the amine solution at 0 °C (ice/H_2O bath). The reaction mixture was allowed to reach rt and

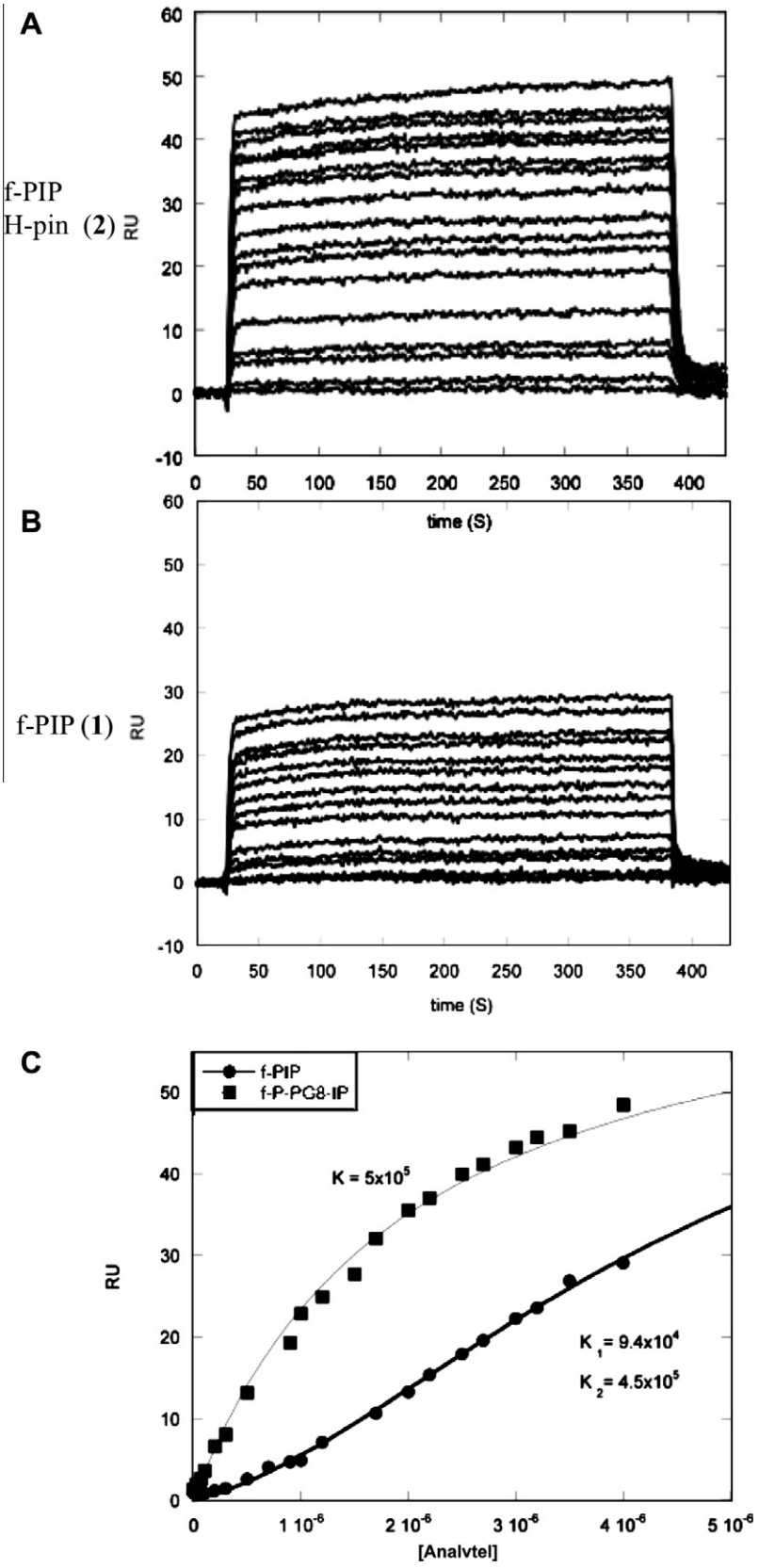

Figure 4. SPR sensorgrams of the cognate sequence, ATCGAT, with (A) H-pin **2** at 0.03, 0.07, 0.1, 0.3, 0.7, 0.9, 1.2, 1.5, 1.7, 2.0, 2.2, 2.5, 2.7, 3.0, 3.2, 3.5, 4.0 μM and (B) f-PIP **1** at 0.1, 0.3, 0.7, 0.9, 1.2, 1.7, 2.0, 2.2, 2.5, 2.7, 3.2, 3.5, 4.0 μM. (C) Steady state plots for sensorgrams given in parts (A) and (B). Non-cognate DNA sequences gave essentially no RUs in their sensorgrams, indicating very weak binding.

was stirred for ~18 h. The reaction was cooled to 0 °C (ice/H_2O bath), was quenched with MeOH, and stirred at 0 °C for ~1 h. The reaction was dissolved in $CHCl_3$ and a basic aqueous work-up was performed.[26] The yellow/cream solid product (**2**) (16 mg,

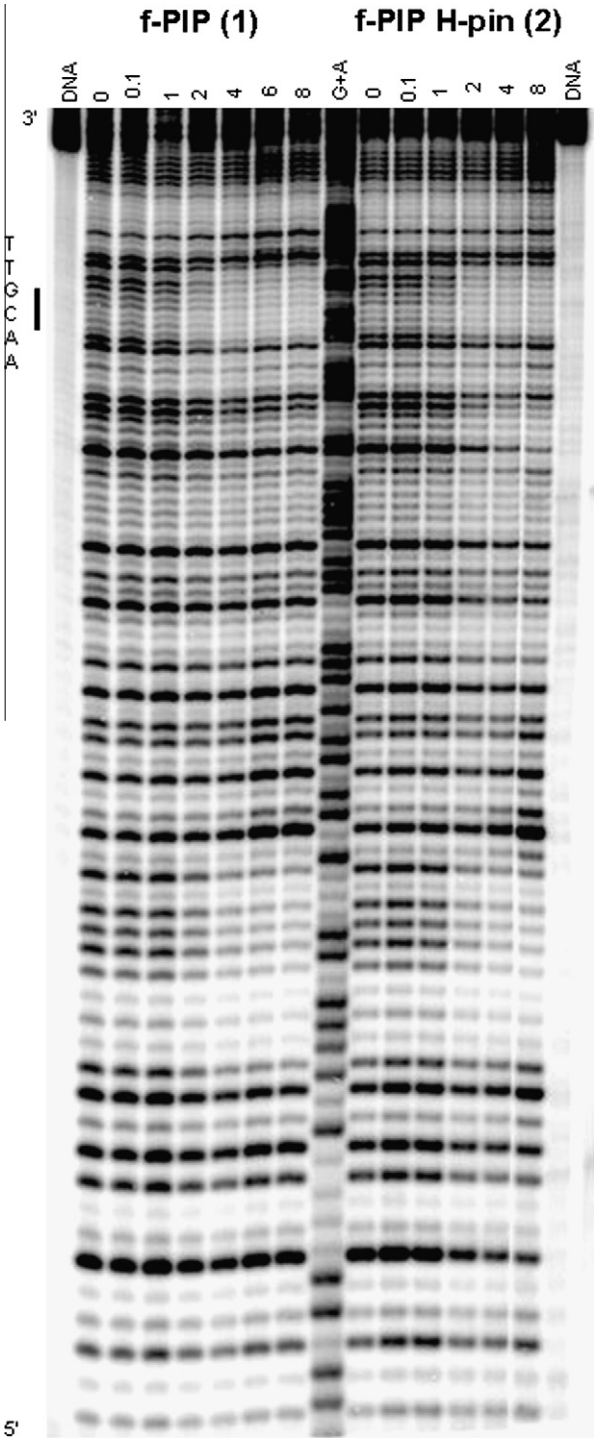

Figure 5. Autoradiograph from DNase I footprinting studies of f-PIP **1** and H-pin **2**.

16%) was isolated by flash column chromatography (silica gel, gradient: 100:0:0–0:100:0–95:4.5:0.5 $CHCl_3$/MeOH/NH_4OH). mp dec at 180 °C: R_f 0.25 (90:10 MeOH/NH_4OH); ^1H NMR: 400 MHz, DMSO-d_6, 10.29 (s, 2H); 10.06 (s, 2H); 9.93 (s, 2H); 8.10 (s, 2H); 7.52 (s, 2H); 7.31 (s, 2H); 7.20 (s, 2H); 6.99 (s, 2H); 6.88 (s, 2H); 4.42 (t, J = 5.0 Hz, 4 H); 3.94 (s, 6H); 3.78 (s, 6H); 3.62 (t, J = 5.4 Hz, 4H); 3.43 (s, 4H); 3.16 (dt, J = 6.4 Hz, 4H); 2.29 (t, J = 6.8 Hz, 4H); 2.12 (s, 12H); 1.59 (quintet, J = 6.8 Hz, 4H); IR (neat) ν 3357, 2924, 2863, 1654, 1650, 1639, 1581, 1537, 1465, 1403, 1381, 1256, 110, 1095 cm^{-1}; MS (ES+) m/z (rel. intensity) 1082 (M+H, 5%); 541 (100%); 361 (52%); HRMS for $C_{50}H_{68}N_{18}O_{10}$ calcd 1081.5444; obsd 1081.5461.

4.2. Thermal denaturation (ΔT_m)

DNA oligomers were purchased from Operon with the following sequences: **ATCGAT**, GAATCGATTGCTCTCAATCGATTC; **TACGAT**, CTACGATTGGTCTTTTTGACCAATC-GTAG; **AAATTT**, CGAAATTTCCCT CTGGAAATTTCG. T_m data were obtained using a Cary 100 Bio (Varian) spectrophotometer with DNA (1 μM) in $PO_4$0 (10 mM Phosphate, 12.5 mM Na^+, 1 mM EDTA, pH 6.2) and compound **2** (3 μM), as previously described.[27]

4.3. Circular dichroism (CD)

CD studies were performed on an OLIS (Bogart, GA) DSM20 spectropolarimeter using a 1 mm pathlength cuvette and a band pass of 2.4 nm as described previously[28] with the exception of the integration time, which was set to integrate as a function of PMT high volts. Experiments were carried out in duplicate using $PO_4$5 buffer (10 mM Phosphate, 50 mM Na^+, 1 mM EDTA, pH 6.2) and the data analyzed using KaleidaGraph software (Synergy Software, Reading, PA).[15]

4.4. Isothermal titration microcalorimetry (ITC)

A VP-ITC microcalorimeter (MicroCal) was used to perform ITC analysis on the DNA sequences described above. Compound **2** was dissolved in $PO_4$5 and the instrument equilibrated at 25 °C. After an initial delay of 300 s, compound **2** (100 μM) was titrated, via 50 injections (3 μL for 7.7 s, repeated every 240 s), into 2 μM DNA ($PO_4$5). The data was analyzed using the same method as previously reported.[29] Origin 7.0 was used to integrate the area under the curve as a function of time. A linear fit was then employed and this was subtracted from the reaction integrations to normalize for non-specific heat components, from which the enthalpy of reaction ΔH was determined.

4.5. Surface plasmon resonance (SPR)

Biosensor chip surface preparations and biotinylated DNA immobilizations were conducted as previously described.[24] The cognate biotin-labeled DNA hairpin used was 5′-biotin-GA**TCGA**TTCTCTAA**TCGA**TTC-3′ (ATCGAT). Similar oligomer design was used for the non-cognate DNAs. The experiments were performed at 25 °C in cacodylic acid buffer at pH 6.25 and 0.1 M NaCl. In a typical experiment, 200 μL samples at different concentrations were injected onto the chip surface with a flow rate of 25 μL/min and 400-s dissociation period. The surface was regenerated with a glycine pH 2.5 solution and multiple buffer injections. The data were fitted with Eq. (1) to obtain macroscopic binding constants:

$$r = (K_1 \times C_{free} + 2 \times K_1 \times K_2 \times C_{free}^2) \,/\, (1 + K_1 \times C_{free} + K_1 \times K_2 \times C_{free}^2) \quad (1)$$

this is used directly for a two site model and with =0 for a one site model of binding.

4.6. Preparation of nuclear cell extracts

Nuclear extracts were prepared using the Active Motif Nuclear-extract kit following the manufacturer's protocol. All steps were carried out at 4 °C in the presence of protease inhibitor mix (Complete; Roche). The protein concentration of the nuclear extract was assayed using the Bio-Rad protein assay.

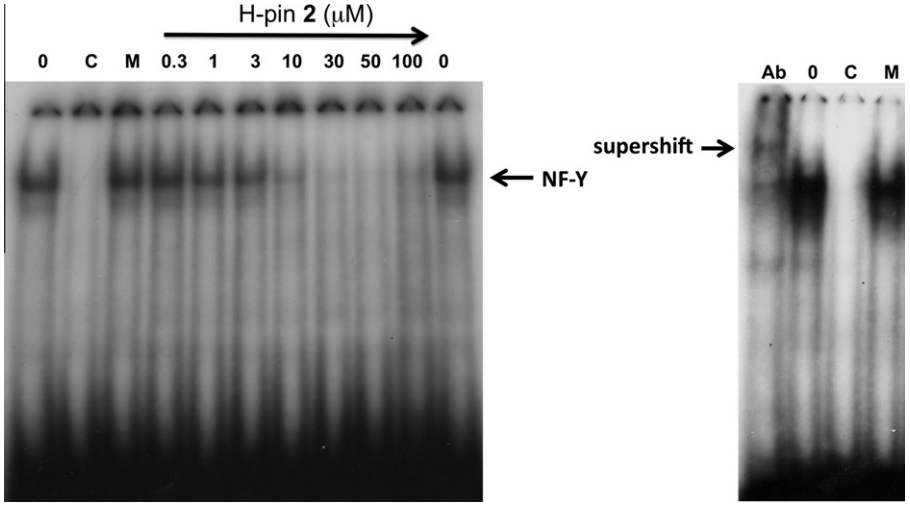

Figure 6. EMSA of H-pin **2** with oligonucleotide containing the ICB2 sequence present on the topoIIα promoter. The oligonucleotide was incubated with 2 (concentrations ranging from 0–50 μM) for 1 h at rt prior to incubation with nuclear extracts from cultured confluent NIH 3T3 cells. Cold (C) and mutated (M) lanes represent reactions carried out in the presence of excess unlabeled and mutated ICB2 oligonucleotides. Lane Ab contains anti-NF-Y(A) antibody and the arrow indicates the band corresponding to the NF-Y bound oligonucleotide. The same nuclear extracts were used under the same experimental conditions in all lanes.

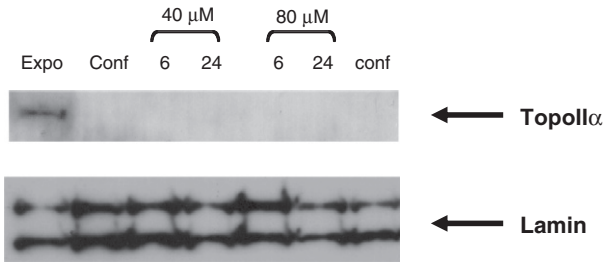

Figure 7. Western blot analysis of NIH 3T3 cell extracts following treatment with H-pin **2**. Cells were either exponentially growing (exp) or maintained at confluence for 96 h (conf). Confluent cells were treated with 40 and 80 μM of **2** and analysis was carried out on samples collected after 6 and 24 h of drug treatment as indicated. Lamin A/C is shown as a loading control.

4.6.1. Electrophoretic mobility shift assay (EMSA)

The oligonucleotides (Eurofins MWG Operon) containing the inverted CCAAT box-2 (ICB2; italicized) used in the EMSA assay are: ICB2 sense 5′-GGCAAGCTAC*GATTGG*TTCTTCTGGACG-3′ and ICB2 antisense 5′-CGTCCAGAAGAA*CCAAT*CGTAGCTTGCC-3′. Oligonucleotides containing a mutated ICB2, with the wild-type ICB2 sequence replaced by AAACC and GGTTT in sense and antisense oligonucleotides respectively were used as specific competitors. Sense and antisense oligonucleotides were annealed in an equimolar ratio. Double-stranded oligonucleotides were 5′-end labeled with T4 Kinase (NEB) using [γ-^{32}P] ATP and subsequently purified on Bio-Gel P-6 columns (Bio-Rad). ~0.1 ng of radiolabeled probe was incubated with **2** for 1 h at room temperature in a total volume of 20 μL containing 4 μL of the 5× binding buffer [20% glycerol, 5 mM $MgCl_2$, 2.5 mM EDTA, 2.5 mM DTT, 250 mM NaCl, and 50 mM Tris–HCl (pH 7.5)], 1 μg poly (dI–dC).poly(dI–dC) (Sigma) and 1× protease inhibitor mix (Complete; Roche). Ten micrograms of nuclear extracts were subsequently added and the reaction was further incubated for another hour. For supershifts, the nuclear extracts were preincubated with an antibody against NF-Y(A) (Abcam) for 1 h, on ice, before addition of the radioactive probe. In competition experiments, radiolabeled probe and competitor were added simultaneously. Prior to loading, 2 μL of loading buffer [25 mmol/L Tris–HCl (pH 7.5), 0.02% Bromophenol blue, and 10% glycerol] was added and the samples were separated on a pre-run 4% polyacrylamide gel in 0.5% TBE buffer containing 2.5% glycerol at 4 °C. After drying the gels, the radioactive signal was visualized by exposure to Fuji medical X-ray film.

4.6.2. Western blot analysis

50 μg of nuclear extract was denatured by heating for 3 min at 95 °C in sample buffer containing 100 mM Tris–Cl (pH 6.8), 4% SDS, 10% 2-mercaptoethanol, 20% glycerol, and 0.02% bromophenol blue. Novex® Sharp Pre-stained molecular weight standards were used as a reference. Proteins were separated on a NuPAGE® 7% Tris-acetate mini-gel (InVitrogen) and subsequently transferred (Trans Blot Cell; Bio-Rad) to polyvinylidene difluoride membranes (Immobilon-P; Millipore). Western blot analysis was performed with the Cell Signaling rabbit polyclonal topoisomerase IIα antibody at a 1:1000 dilution using an enhanced chemiluminescence Western blot detection kit and protocol (Amersham) using 5% bovine serum albumin (Promega) as blocking reagent and TBS-0.1% Tween-20 (BDH) as a buffer. The chemiluminescent signal was visualized by exposing the blots to Fuji medical X-ray film.

4.6.3. DNase I footprinting studies

A radiolabeled DNA fragment of 131 base pairs containing a unique cognate site 5′-AACGTT-3′ was generated by polymerase chain reaction as described previously.[30] The amplified fragment was purified on a Bio-Gel P-6 column followed by agarose gel electrophoresis and isolated using the Mermaid Kit (MP biomedicals) according to the manufacturer's instructions.

DNase I digestions were conducted in a total volume of 8 μL. The labeled DNA fragment (2 μL, 200 counts s^{-1}) was incubated for 30 min at room temperature in 4 μL TN binding buffer (10 mM Tris Base, 10 mM NaCl, pH 7) containing the required drug concentration. Cleavage by DNase I was initiated by addition of 2 μL of DNase I solution (20 mM NaCl, 2 mM $MgCl_2$, 2 mM $MnCl_2$, DNase I 0.02 U, pH 8.0) and stopped after 3 min by snap freezing the samples on dry ice. The samples were subsequently lyophilized to dryness and resuspended in 5 μL of formamide loading dye (95% formamide, 20 mM EDTA, 0.05% bromophenol blue, and 0.05% cyanol blue). Following heat denaturation for 5 min at 90 °C, the samples were loaded on a denaturing polyacrylamide (10%) gel (Sequagel, National Diagnostics, UK) containing urea (7.5 mM). Electrophoresis was carried out for 2 h at 1650 V (~70 W, 50 °C) in 1× TBE buffer. The gel was then transferred onto Whatman

3MM and dried under vacuum at 80 °C for 2 h. The gel was exposed overnight to Fuji medical X-ray film and developed on a Konica Medical Film Processor SRX-101A.

4.7. Cytotoxicity studies

B16 and L1210 cell line maintenance and MTT assays were conducted as previously reported,[31] with the exception of incubation in a 10% humidified CO_2 atmosphere (cf. 5%).

Acknowledgments

Support from the NSF (CHE 0550992) and CRUK (C2259/A9994) is greatly acknowledged. A.F. thanks the Eli Lilly Co. for a summer research fellowship.

Supplementary data

Supplementary data associated with this article can be found, in the online version, at doi:10.1016/j.bmc.2010.06.041.

References and notes

1. Melander, C.; Burnett, R.; Gottesfeld, J. M. *J. Biotechnol.* **2004**, *112*, 195.
2. Kopka, M. L.; Goodsell, D. S.; Han, G. W.; Chiu, T. K.; Lown, J. W.; Dickerson, R. E. *Structure* **1997**, *5*, 1033.
3. Le, N. M.; Sielaff, A. M.; Cooper, A. J.; Mackay, H.; Brown, T.; Kotecha, M.; O'Hare, C.; Hochhauser, D.; Lee, M.; Hartley, J. A. *Bioorg. Med. Chem. Lett.* **2006**, *16*, 6161.
4. Ronchi, A.; Bellorini, M.; Mongelli, N.; Mantovani, R. *Nucleic Acids Res.* **1995**, *23*, 4565.
5. Isaacs, R. J.; Harris, A. L.; Hickson, I. D. *J. Biol. Chem.* **1996**, *271*, 16741.
6. Tolner, B.; Hartley, J. A.; Hochhauser, D. *Mol. Pharmacol.* **2001**, *59*, 699.
7. Hochhauser, D.; Kotecha, M.; O'Hare, C.; Morris, P. J.; Hartley, J. M.; Taherbhai, Z.; Harris, D.; Forni, C.; Mantovani, R.; Lee, M.; Hartley, J. A. *Mol. Cancer Ther.* **2007**, *6*, 346.
8. Henry, J. A.; Le, N. M.; Nguyen, B.; Howard, C. M.; Bailey, S. L.; Horick, S. M.; Buchmueller, K. L.; Kotecha, M.; Hochhauser, D.; Hartley, J. A.; Wilson, W. D.; Lee, M. *Biochemistry* **2004**, *43*, 12249.
9. Buchmueller, K. L.; Staples, A. M.; Howard, C. M.; Horick, S. M.; Uthe, P. B.; Le, M. N.; Cox, K. K.; Nguyen, B.; Pacheco, K. A. O.; Wilson, W. D.; Lee, M. *J. Am. Chem. Soc.* **2005**, *127*, 742.
10. O'Hare, C.; Uthe, P.; Mackay, H.; Blackmon, K.; Jones, J.; Brown, T.; Nguyen, B.; Wilson, W. D.; Lee, M.; Hartley, J. A. *Biochemistry* **2007**, *46*, 11661.
11. (a) Dwyer, T. J.; Geierstanger, B. H.; Mrksich, M.; Dervan, P. B.; Wemmer, D. E. *J. Am. Chem. Soc.* **1993**, *115*, 9900; (b) Mrksich, M.; Dervan, P. B. *J. Am. Chem. Soc.* **1993**, *115*, 9892; (c) Mrksich, M.; Dervan, P. B. *J. Am. Chem. Soc.* **1994**, *116*, 3663; (d) Olenyuk, B.; Jitianu, C.; Dervan, P. B. *J. Am. Chem. Soc.* **2003**, *125*, 4741; (e) Dervan, P. B. *Bioorg. Med. Chem.* **2001**, *9*, 2215.
12. (a) Al-Said, N. J.; Lown, W. *Synth. Commun.* **1995**, *25*, 1059; (b) Chen, Y.-H.; Yang, Y. J.; Lown, W. *J. Biomol. Struct. Dyn.* **1996**, *14*, 341; (c) Chen, Y.-H.; Liu, J.-X.; Lown, J. W. *Bioorg. Med. Chem. Lett.* **1995**, *5*, 2223; (d) O'Hare, C. C.; Mack, D.; Tandon, M.; Sharma, S. K.; Lown, J. W.; Kopka, M. L.; Dickerson, R. E.; Hartley, J. A. *Proc. Natl. Acad. Sci.* **2002**, *99*, 72.
13. Brown, T.; Taherbhai, Z.; Sexton, J.; Sutterfield, A.; Turlington, M.; Jones, J.; Stallings, L.; Stewart, M.; Buchmueller, K.; Mackay, H.; O'Hare, C.; Kluza, J.; Nguyen, B.; Wilson, D.; Lee, M.; Hartley, J. A. *Bioorg. Med. Chem.* **2007**, *15*, 474.
14. *Advanced Organic Chemistry: Reactions, Mechanisms and Structure*; March, J., Ed., 4th ed.; John Wiley & Sons: New York, 1992; p 392.
15. Lacy, E. R.; Le, N. M.; Price, C. A.; Lee, M.; Wilson, W. D. *J. Am. Chem. Soc.* **2002**, *124*, 2153.
16. (a) Lyng, R.; Rodger, A.; Norden, B. *Biopolymers* **1991**, *31*, 1709; (b) Lyng, R.; Rodger, A.; Norden, B. *Biopolymers* **1992**, *32*, 1201.
17. Yang, X.-L.; Kaenzig, C.; Lee, M.; Wang, A. *Eur. J. Biochem.* **1999**, *263*, 646.
18. Lee, M.; Krowicki, K.; Hartley, J. A.; Pon, R. T.; Lown, J. W. *J. Am. Chem. Soc.* **1988**, *110*, 3641.
19. Mackay, H.; Brown, T.; Sexton, J. S.; Uthe, P. B.; Westrate, L.; Sielaff, A.; Jones, J.; Lajiness, J. P.; Kluza, J.; O'Hare, C. C.; Nguyen, B.; Davies, Z.; Bruce, C.; Wilson, W. D.; Hartley, J. A.; Lee, M. *Bioorg. Med. Chem.* **2008**, *16*, 9145.
20. Wilson, W. D.; Tanious, F. A.; Fernandez-Saiz, M.; Ted Rigl, C.. In *Drug–DNA Interaction Protocols (Methods in Molecular Biology)*; Fox, K., Ed.; Humana Press: Totowa, 1997; Vol. 90, pp 219–240.
21. Mackay, H.; Brown, T.; Sexton, J. S.; Kotecha, M.; Nguyen, B.; Wilson, W. D.; Kluza, J.; Savic, B.; O'Hare, C.; Hochhauser, D.; Lee, M.; Hartley, J. A. *Bioorg. Med. Chem.* **2008**, *16*, 2093.
22. Chaires, J. B. *Annu. Rev. Biophys.* **2008**, *37*, 135.
23. Chellani, M. *Am. Biotechnol. Lab.* **1999**, *17*, 14.
24. Nguyen, B.; Tanious, F. A.; Wilson, W. D. *Methods* **2008**, *42*, 150.
25. (a) Nishijima, S.; Shinohara, K.; Bando, T.; Minoshima, M.; Kashiwazaki, G.; Sugiyama, H. *Bioorg. Med. Chem.* **2010**, *18*, 978; (b) Nickols, N. G.; Jacobs, C. S.; Farkas, M. E.; Dervan, P. B. *Nucleic Acids Res.* **2007**, *35*, 363; (c) Edelson, B. S.; Best, T. P.; Olenyuk, B.; Nickols, N. G.; Doss, R. M.; Foister, S.; Heckel, A.; Dervan, P. B. *Nucleic Acids Res.* **2004**, *32*, 2802; (d) Best, T. P.; Edelson, B. S.; Nickols, N. G.; Dervan, P. B. *Proc. Natl. Acad. Sci. U.S.A.* **2003**, *100*, 12063.
26. Basic aqueous work-up refers to washing the organic layer with a solution of aq NaOH (pH ~11). The aqueous layer was then back-extracted with $CHCl_3$ (×3). The organic layers were then combined, dried (Na_2SO_4) and evaporated to dryness.
27. Flores, L. V.; Staples, A. M.; Mackay, H.; Howard, C. M.; Uthe, P. B.; Sexton, J. S.; Buchmueller, K. L.; Wilson, W. D.; O'Hare, C.; Kluza, J.; Hochhauser, D.; Hartley, J. A.; Lee, M. *ChemBioChem* **2006**, *7*, 1722.
28. Sielaff, A. S.; Mackay, H.; Brown, T.; Lee, M. *Biochem. Biophys. Res. Commun.* **2008**, *369*, 630.
29. Buchmueller, K. L.; Bailey, S. L.; Matthews, D. A.; Taherbhai, Z. T.; Register, J. K.; Davis, Z. S.; Bruce, C. D.; O'Hare, C.; Hartley, J. A.; Lee, M. *Biochemistry* **2006**, *45*, 13551.
30. O'Hare, C. C.; Uthe, P.; Mackay, H.; Blackmon, K.; Jones, J.; Brown, T.; Nguyen, B.; Wilson, W. D.; Lee, M.; Hartley, J. A. *Biochemistry* **2007**, *46*, 11661.
31. LeBlanc, R.; Dickson, J.; Brown, T.; Stewart, M.; Pati, H. D.; VanDerveer, D.; Arman, H.; Harris, J.; Pennington, W.; Holt, H. L., Jr.; Lee, M. *Bioorg. Med. Chem.* **2005**, *13*, 6025.